Journal of Power Sources 200 (2012) 1–7

Contents lists available at SciVerse ScienceDirect

Journal of Power Sources

journal homepage: www.elsevier.com/locate/jpowsour

Preparation and performance of sulfonated polyimide/Nafion multilayer membrane for proton exchange membrane fuel cell

Chao-Chieh Lin[a], Wan-Fu Lien[b,*], Yen-Zen Wang[a], Hung-Wei Shiu[a], Chi-Hung Lee[a]

[a] Department of Chemical Engineering and Materials Engineering, National Yunlin University of Science and Technology, Yunlin 64002, Taiwan, ROC
[b] Department of Cultural Heritage Conservation, National Yunlin University of Science and Technology, Yunlin 64002, Taiwan, ROC

ARTICLE INFO

Article history:
Received 29 June 2011
Received in revised form 2 October 2011
Accepted 3 October 2011
Available online 1 November 2011

Keywords:
Sulfonated polyimide
Nafion
Multilayer membrane
Fuel cell
Durability

ABSTRACT

A novel and simple thermal imidization method is used to prepare the sulfonated polyimide/Nafion multilayer (NF-SPI-NF) membrane from sulfonated polyimide (SPI) and Nafion-containing solution (Na^+ form). The NF-SPI-NF membrane is prepared by immersing a sulfonated poly(amic acid) (SPAA) membrane into the Nafion-containing solution followed by thermal imidization via solvent evaporation. This Nafion is firmly adhered to either side of the SPI membrane via thermal imidization. The prepared membranes are characterized by Fourier transform infrared spectroscopy (FT-IR), thermogravimetric analysis (TGA) and proton conductivity. The membranes are immersed in Fenton's reagent at room temperature to test their oxidative stability and the durability of a single proton exchange membrane fuel cell (PEMFC) system. Analytical results show a marked improvement in NF-SPI-NF membrane stability by adding Nafion layer comparing with that of native SPI membrane. The performance of PEMFC with the NF-SPI-NF membrane is similar to that of PEMFC with the commercially available Nafion 212 at 70 °C.

1. Introduction

Under increased environmental concern, proton exchange membrane fuel cell (PEMFC) have attracted considerable interest as clean energy sources for transportable, stationary, and portable power applications due to their high efficiency and low environmental pollution [1,2]. Notably, a proton exchange membrane (PEM) is a key component in PEMFC systems and functions as a proton conductor and fuel separator between an anode and cathode. Perfluorosulfonate ionomers (PFSI), such as DuPont's Nafion membranes, are commercially available and have the advantages of high proton conductivity, excellent chemical stability, and long-term stability. However, they have limited industrial applications due to their high cost, high gas permeability, operating temperature less than 80 °C, and the environmental inadaptability of fluorinated materials [3,4]. Over the last decade, various proton conductive materials have been developed as alternative membranes. Sulfonated polyimide with a six-member imide ring is considered a promising candidate due to its excellent thermal stability, high mechanical strength, and good film forming ability. Mercier et al. [5–7] first applied sulfonated polyimide (SPI) derived from 1,4,5,8-naphthalenetetracarboxylic dianhydride (NTDA), 2,2′-benzidinedisulfonic acid (BDSA), and a nonsulfonated diamine (such as 4,4′-oxydianiline (ODA)). Although SPIs have many advantages, the different surfaces and bulk properties between hydrocarbon membranes and the PFSI binder typically cause low compatibility, forming unstable interfaces in membrane electrode assemblies (MEAs) [8]. Poor durability under fuel cell operating conditions is also major drawback of these hydrocarbon polymers. Jiang et al. [9] utilized sulfonated poly(ether ether ketone) (SPEEK) membranes with a low degree of sulfonation as support material in preparing Nafion/SPEEK/Nafion (NSN) multilayer membranes. The NSN multilayer membrane was prepared using a casting procedure in the solution condition. The NSN multilayer membrane had better cell performance than native Nafion in direct methanol fuel cell (DMFC) system. However, after tested in DMFC system for 3 weeks, two Nafion outer layers separated from the SPEEK central layer, likely due to incompatibility and poor interlayer bonding between Nafion and SPEEK. Wang et al. [10] also prepared a Nafion/sulfonated polyimide/Nafion multilayer membrane by immersing the sulfonated polyimide (SPI) into the Nafion-containing solution. The stability of the multilayer membrane improved markedly after adding the Nafion layer compared with that of the SPI membrane. However, the multilayer membrane was prepared via the coating method, which cannot generate strong interlayer bonding between Nafion and the SPI membrane. To enhance interfacial stability, Sung et al. [11] coated crosslinkable materials on a sulfonated polyimide membrane, these materials were crosslinked at the interface during the hot-pressing process for MEA. With enhanced interfacial adhesion, the new MEA with the crosslinked layer maintained a stable interface after long-term operation compared to that of the MEA without a crosslinked

* Corresponding author. Tel.: +886 5 534 2601x3171; fax: +886 5 531 2176.
E-mail address: lienwf@yuntech.edu.tw (W.-F. Lien).

0378-7753/$ – see front matter © 2011 Published by Elsevier B.V.
doi:10.1016/j.jpowsour.2011.10.001

layer. However, introducing a crosslinkable layer degraded cell performance because most catalyst particles were covered by the crosslinked layer.

This work, developed a novel multilayer membrane by immersing sulfonated poly(amic acid) (SPAA) into Nafion-containing solution. The Nafion coated SPAA membrane was dried in an oven to remove residual solvents and to imidize the SPAA into SPI. The Nafion firmly adhered to either side of the SPI membrane. Proton conductivity, membrane properties, and single cell performance of the multilayer membrane were investigated.

2. Experimental

2.1. Materials

1,4,5,8-Naphthalenetetracarboxylic dianhydride (NTDA, 95% pure; Aldrich) was dried under vacuum before use. 4,4′-Oxydianiline (ODA, 98% pure; Aldrich) was used without further purification. 2,2′-Benzidinedisulfonic acid (BDSA, 70% pure; TCI) was dissolved in ethanol and was neutralized with triethylamine (TEA, 99.9% pure; Sigma–Aldrich) at 60 °C. BDSA was purified by recrystallization from the ethanol solution and was dried under vacuum for three days. Benzoic acid (BA, 99.5% pure; Sigma–Aldrich) and Nafion-containing solution (Nafion® PFSA polymer dispersions, 5 wt.%, DuPont Fuel Cells) were used without further purification. In order to prevent the crosslinking reaction between sulfonic groups, Nafion ($-SO_3^-H^+$) was reacted with NaCl to form the sulfonic salt ($-SO_3^-Na^+$). *m*-Cresol (99% pure; Sigma–Aldrich) and TEA were used without further purification.

2.2. Synthesis of the sulfonated polyimide/Nafion multilayer membrane

The sulfonated polyimide/Nafion multilayer (NF-SPI-NF) membrane was synthesized using a two-step method (Scheme 1). The SPI-NF multilayer membrane was prepared by immersing sulfonated poly(amic acid) (SPAA) into the Nafion-containing solution followed by thermal imidization during solvent evaporation. Synthesis of SPAA with a molar ratio of NTDA:BDSA–Et_3N:ODA of 1.0:0.6:0.4 was performed as follows. In total, 1.08 g (2 mmol) BDSA–E_3tN and 0.6 g (3 mmol) ODA were dissolved in 20 mL *m*-cresol in a 100 mL three-necked flask. The solution was then stirred with a magnetic stirrer under nitrogen atmosphere. Finally, 1.34 g (5 mmol) NTDA and 1.22 g (10 mmol) benzoic acid were introduced and the mixture was stirred under ambient temperature for a few minutes and then heated at 80 °C overnight, the solution was then poured into acetone. The fiber-like precipitate was filtered off, washed thoroughly with acetone, and dried in a vacuum at 80 °C for 15 h. The SPAA (in triethylamine salt form) was dissolved in *m*-cresol (5 wt.%), and the solution was cast onto glass plates and dried in air at 80 °C for 12 h. A flexible SPAA membrane was then obtained and removed from the glass plate, and then immersed in a Nafion-containing solution (Na^+ form). The Nafion coated SPAA membrane was dried in an oven at 60 °C for 6 h to remove residual solvents and at 180 °C for 24 h to imidize the SPAA into SPI. The NF-SPI-NF multilayer membrane was formed. The Nafion side layer was 3–5 μm in thickness. The prepared membranes were soaked in 1 M H_2SO_4 at room temperature for 12 h. These membranes were then thoroughly washed with de-ionized water.

2.3. Polymer characterization

2.3.1. Fourier transform infrared spectroscopy and ion exchange capacity

The prepared membranes were tested by Fourier transform infrared (FT-IR) spectroscopy with attenuated total reflection (ATR) form (Perkin Elmer Spectrum One). A minimum of 8 scans were signal-averaged with a resolution of 2 cm^{-1} in the 4000–650 cm^{-1} range. The ion exchange capacity (IEC) was measured using the classical titration method. The dry membranes were soaked in a saturated NaCl solution. Released protons were titrated using 0.1 M NaOH solution. The IEC value was recorded as an average value for each sample in milliequivalent NaOH per gram polymer (mequiv. g^{-1}).

2.3.2. Measurements of water uptake and dimensional change

The water absorption values of SPI, Nafion, and NF-SPI-NF membranes were determined at 30 °C. These membranes were dried in a vacuum at 100 °C for 24 h, and then weighed and immersed in deionized water at room temperature for 24 h. Wet membranes were dried by wipe and immediately weighed again. The water uptake (WU) of membranes was calculated based on weight percentage, as Eq. (1):

$$\mathrm{WU} = \frac{W_{\mathrm{wet}} - W_{\mathrm{dry}}}{W_{\mathrm{dry}}} \times 100\% \tag{1}$$

where W_{wet} and W_{dry} are the weights of corresponding water-swollen and dry membranes, respectively.

Dimensional change of membranes was investigated by immersing round samples into water at room temperature for a given duration. The changes in thickness and diameter were defined as Eq. (2):

$$\begin{aligned} \Delta l_{\mathrm{c}} &= \frac{l_{\mathrm{w}} - l_{\mathrm{d}}}{l_{\mathrm{d}}} \\ \Delta t_{\mathrm{c}} &= \frac{t_{\mathrm{w}} - t_{\mathrm{d}}}{t_{\mathrm{d}}} \end{aligned} \tag{2}$$

where t_{d} and l_{d} are the thickness and diameter of the membrane dried in a vacuum at 100 °C for 24 h, respectively; and t_{w} and l_{w} refer to membrane immersed in deionized water at room temperature for 24 h.

2.3.3. Thermal analysis

Thermogravimetric analysis (TGA) (TA Instruments-Q500) was performed to estimate the thermal stability of dry membranes and water weight loss of wet membranes. The temperature was heated to 900 °C at the rate of 10 °C min^{-1} under nitrogen atmosphere. The weight of sample is about 5–10 mg.

2.3.4. Proton conductivity

Transverse proton conductivities of membranes were measured by an AC impedance analyzer (Autolabe PGSTA30) over a frequency range of 1–10,000 kHz. The membranes, roughly 40–60 μm in thickness, were sandwiched between two stainless steel electrodes, and placed in an open, temperature-controlled cell. Films were preliminarily hydrated by immersion in room-temperature water for 2 h.

Conductivity σ in the transverse direction was calculated from impedance data, as Eq. (3):

$$\sigma = \frac{d}{RA} \tag{3}$$

where d and A are the thickness and surface area of the membrane sample, respectively, and R is resistance. Proton conductivities of membranes were also measured as a function of temperature (30–80 °C) in deionized water.

2.3.5. Oxidative stability

A small piece of membrane sample (30–40 mg) was soaked in Fenton's reagent (30 ppm $FeSO_4$ in 30% H_2O_2) at 25 °C. Stability was evaluated by recording the time when membranes became a

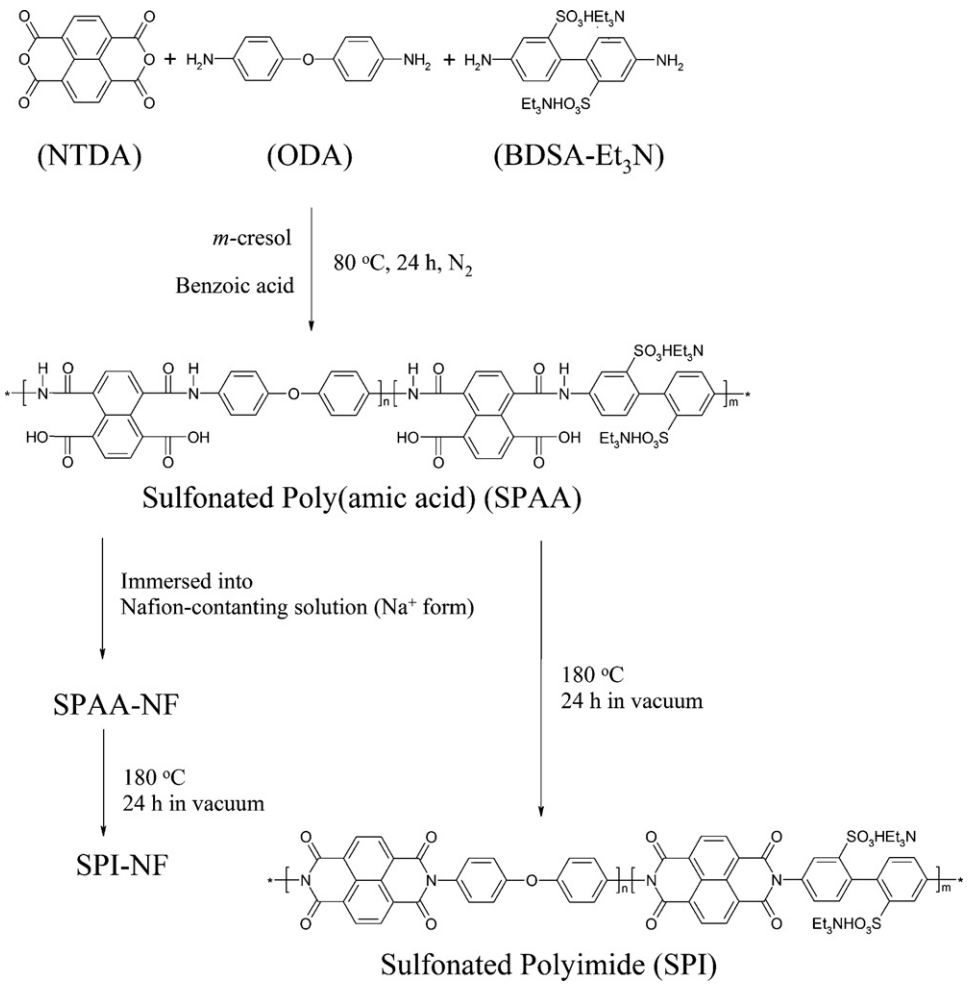

Scheme 1. Synthesis of SPI and SPI-NF.

little brittle (time1 = τ_1) and completely dissolved in the reagent (time2 = τ_2) [12].

2.3.6. Morphological analysis

The cross-sectional morphology of the SPI-NF multilayer membrane was examined by Field Emission Scanning Electron Microscope (FE-SEM) (JEOLJSM-7401F).

2.4. Preparation and evaluation of the membrane electrode assembly

To fabricate an membrane electrode assembly (MEA) for PEMFC, a 5 wt.% Nafion solution (136.2 mg) and a 20 wt.% Pt/C (E-TEK) (12.6 mg) were mixed with isopropyl alcohol in a beaker. The Pt/C catalyst loading on the anode and cathode was 0.5 mg Pt per cm^2. An MEA was prepared by hot-pressing the electrode/membrane/electrode into a sandwich at 140 °C for 5 min under 50 kgf cm^{-2}. The MEA was put in a single-cell test equipment (active area, 5 cm^2) (Asia Pacific Fuel Cell Technologies, Ltd.), and then was installed in a fuel cell test station (model FCED-P50; Asia Pacific Fuel Cell Technologies, Ltd.). The follow rate of reactant gases (H_2 and O_2) and single-cell temperature can be changed in this fuel cell test station. The humidifier gas temperature and cell temperature of the PEMFC were maintained at 30 °C, and 70 °C, using H_2 and O_2 at feed rates of 100 and 200 mL min^{-1}, respectively, with a bulk gas pressure of 0.3 MPa.

To test the durability of the cells with Nafion 212, SPI and SPI-NF membranes, cells were measured at a constant current density of 200 mA cm^{-2}, and at 30 °C under a humidified condition. The flow rates of inlet gases were maintained at 100 mL min^{-1} and 200 mL min^{-1} for H_2 and O_2, respectively. Cell voltage was monitored during operation.

3. Results and discussion

3.1. Synthesis and characterization of the SPI-NF membrane

A novel and simple thermal imidization method was applied to prepare the SPI/Nafion multilayer (NF-SPI-NF) membrane from an sulfonated poly(amic acid) and Nafion-containing solution (the Na^+ form). The NF-SPI-NF membrane was prepared by immersing the SPAA membrane into Nafion solution followed by solvent evaporation and imidization as shown in Scheme 1. The Nafion film was firmly anchored on both sides of the SPI membrane via the interpenetration effect. In other words, the boundary between SPI and Nafion disappeared after interpenetration, and Nafion successfully adhered to the SPI membrane.

The SPI was created as an ionomer with an ion exchange capacity (IEC) value of 1.88 mequiv. g^{-1}. This IEC value is close to its theoretical value of 1.90 mequiv. g^{-1}, indicating that copolymerization was successful and sulfonate groups were introduced into polymers.

The SPI-NF multilayer membrane in its proton form was characterized by FT-IR spectra. Fig. 1 shows the FT-IR spectra of SPI, NF-SPI-NF, and Nafion 212 membranes. The strong absorption bands around 1714 cm^{-1} (ν_{as} (C=O)), 1673 cm^{-1} (ν_s (C=O)), and

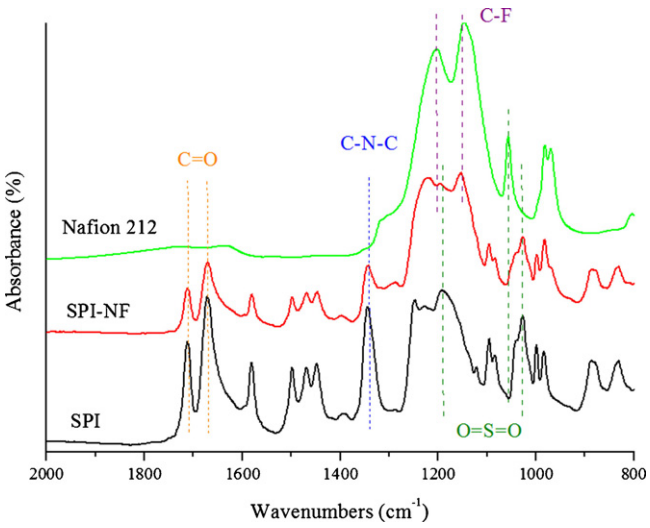

Fig. 1. FT-IR spectra of the SPI, SPI-NF and Nafion 212 membranes.

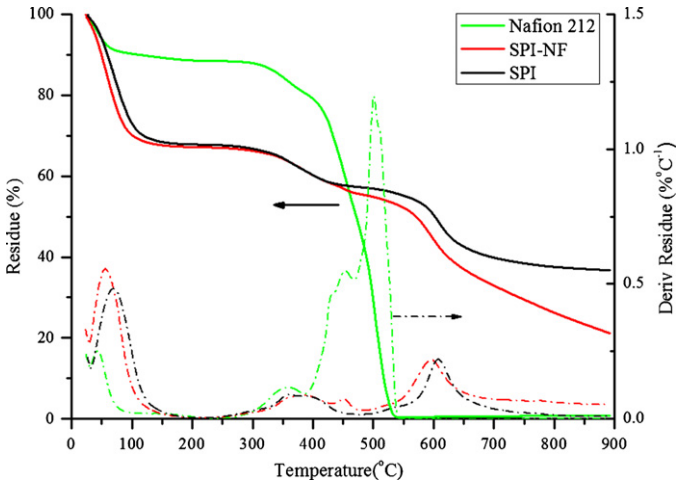

Fig. 2. TGA thermograms of the SPI, SPI-NF and Nafion 212 membranes.

1347 cm^{-1} (ν(C–N–C, imide)) were assigned to naphthalenic imide rings [13]. The asymmetrical and symmetrical vibrations of the O=S=O groups in sulfonic acid groups were at 1197 cm^{-1} and 1026 cm^{-1}, respectively [13]. Complete imidization was supported by the absence of an absorbance peak at around 1780 cm^{-1}, which was assigned to carbonyl groups in anhydride rings. The characteristic peaks from fluoroethylenes of Nafion 212 were at 1203 cm^{-1} and 1145 cm^{-1}, and were assigned to the asymmetrical and symmetrical F–C–F stretching vibration, respectively [14]. The higher acidity sulfonic acid group of Nafion appeared at 1056 cm^{-1} [14].

3.2. Thermal properties

The thermal stability of the SPI, SPI-NF, Nafion 212 membranes were analyzed using their TGA thermograms (Fig. 2), which indicate that all membranes exhibited a three-step weight loss in nitrogen atmosphere. The first weight loss occurred at temperatures less than 200 °C due to loss of water molecules absorbed by the highly hydrophilic $-SO_3H$ groups [15]. The second weight loss was at roughly 300 °C, and was attributed to decomposition of sulfonic acid groups [12]. The third weight loss, at roughly 550 °C, was due to the breaking down of SPI backbone. The weight loss of the NF-SPI-NF at around 380–400 °C appeared more clearly than that of the SPI due to the Nafion backbone breaking down as shown in Fig. 2.

Fig. 2 also shows the derivative thermogram (DTG). For the NF-SPI-NF membrane, the second stage of weight loss at roughly 450 °C, which is higher than that of the SPI membrane, was due to the thermo weight loss of Nafion pieces, indicating that the interpenetration effect between SPI and Nafion enhanced adhesion. The SPI-NF has superior thermal properties and can be utilized as polymer electrolyte membranes for high temperature operating conditions.

3.3. Properties of membrane

The water content in sulfonated polymers has an important role in the transport of protons across membranes. In a fully hydrated state, sulfonated polymers can dissociate to produce immobile sulfonic acid groups and mobile protons in an aqueous solution. The free protons moved through a localized ionic network within fully water-swollen sulfonated polymer membranes. Accordingly, suitable water content should be maintained in sulfonated polymer membrane to ensure high proton conductivity. Table 1 lists the water content in SPI, SPI-NF, and Nafion 212 membranes. Experimental results show that the SPI-NF membrane had a absorbed slightly more water than the SPI membrane, indicating that securely adhered Nafion on either side of the SPI membrane can help keep absorbed water within the SPI-NF membrane.

Table 1 lists the proton conductivity of the SPI, NF-SPI-NF, and Nafion 212 membranes. The proton conductivity of the NF-SPI-NF membrane was higher than that of the SPI membrane, proving that the Nafion layers were securely adhered to SPI. The Nafion will increase the conductivity of SPI.

The SPI, and NF-SPI-NF membranes had anisotropic swelling with a larger change in the thickness than in the plane direction. Anisotropic membrane swelling is due to the polymer chain aligned in the plane direction [13].

3.4. Stability

Oxidative stability was characterized by the time needed for test membranes to break down and dissolve completely. The NF-SPI-NF membrane had better oxidative stability than the SPI membrane

Table 1
Ion exchange capacity, water uptake, dimensional change, proton conductivity, and oxidative stability of proton exchange membranes.

Code	IEC (mequiv. g^{-1})[a]	WU (%)[b]	Proton conductivity (mS cm^{-1})[c]		Dimensional change		Oxidative stability[d]	
			30 °C	80 °C	Δt_d (%)	Δl_d (%)	τ_1 (h)	τ_2 (h)
SPI	1.90	35.0	79	160	25.0	7.2	49	68
SPI-NF	–	37.5	95	165	25.0	8.7	73	110
Nafion 212	0.92	23.0	120	160	20.0	2.5	>80	–

[a] Determined from potentiometric titration.
[b] Measured at 50 °C.
[c] Measured in water.
[d] At 30 °C in 30% H_2O_2 containing 30 ppm $FeSO_4$.

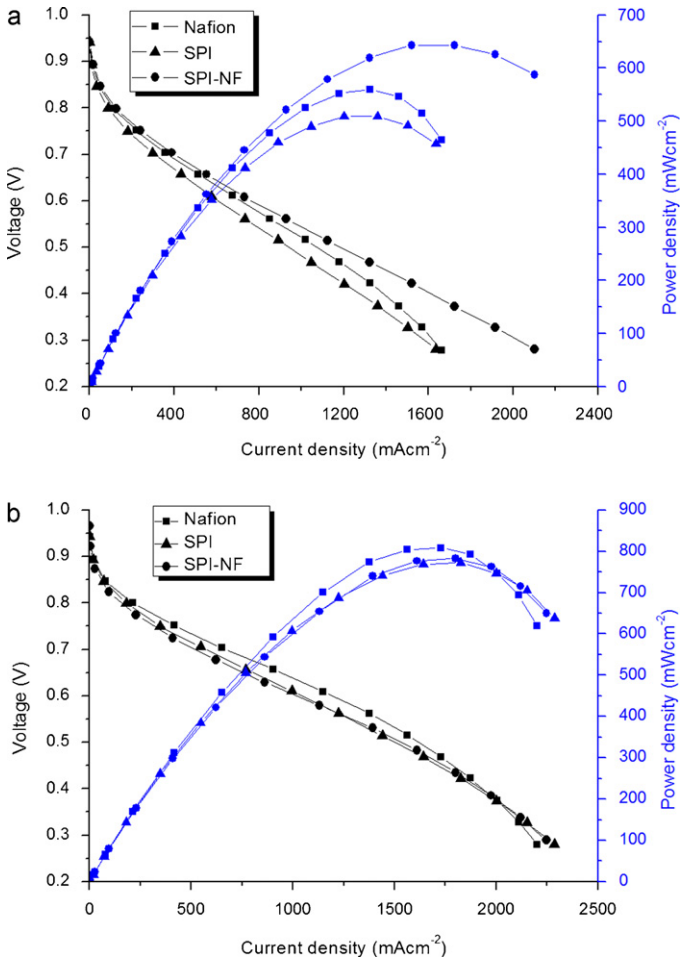

Fig. 3. Polarization and power density curves for three MEAs equipped with SPI, SPI-NF, and Nafion 212 membrane under humidified condition: (a) at 30 °C and (b) at 70 °C.

(Table 1), because Nafion has structure resembling that of Teflon, which resists oxidation by carrying a lot of C–F bonds [16]. Therefore, the Nafion layer on either side of the SPI membrane effectively improved oxidative stability.

3.5. Performance of the PEMFC under humidified condition

Fig. 3 shows the thermal effects (30 °C, and 70 °C) on a single cell with the SPI, SPI-NF, and Nafion 212 membranes, under H_2/O_2 at 100/200 mL min^{-1} and at the same temperature for humidification of gases and the cell. Table 2 lists the PEMFC performance data for the open circuit voltage (OCV), cell voltage at current density of 1.0 A cm^{-2} ($V_{1.0}$), maximum power density (W_{max}), through-plane proton conductivity ($\sigma_{\perp,FC}$), and resistance (R). Fig. 3(a) shows the performance of PEMFC with the SPI, NF-SPI-NF, and Nafion 212 membranes at 30 °C. The cell performance of NF-SPI-NF and Nafion 212 membranes had outstanding and better than that of SPI membrane. The maximum power density of PEMFC with NF-SPI-NF membrane was 626 mW cm^{-2}, which is higher than that of PEMFC with SPI and Nafion 212 membranes. This was because the high IEC value (1.90 mequiv. g^{-1}) of SPI layer provided more complete proton conduction pathway at 30 °C. The polarization curve of PEMFC with SPI membrane had a larger voltage drop than that of PEMFC with other membranes up to 1.0 A cm^{-2}, indicating that the SPI membrane had higher activation and ohmic loss. The SPI membrane may have large interfacial resistance because of poor adhesion between the SPI membrane and catalyst electrode, resulting in worse cell performance than the other membranes. Notably, the through-plane proton conductivity ($\sigma_{\perp,FC}$) under PEMFC operation (Table 2) reflects cell performance behavior. Increased temperature improved reaction kinetics and membrane conductivity, reported in literature [17–19]. Fig. 3(b) shows the performance of PEMFC with the SPI, NF-SPI-NF, and Nafion 212 membranes at 70 °C. Cell performance of PEMFC with the NF-SPI-NF membrane was as good as that of PEMFC with the commercial Nafion 212 membrane. The maximum power density of the PEMFC with NF-SPI-NF membrane was 763 mW cm^{-2}, similar to that of the PEMF with Nafion 212 membrane (768 mW cm^{-2}). In high current density region, potential loss is due to mass transport limitations, which can be associated with the diffusion problem of reactant gases. This diffusion problem is due to water accumulation caused by crossover and production via oxygen reduction, which made reactant gases more difficult to reach the electrode catalyst sites as shown in Fig. 3(b). Water flooding is more serious for PEMFC with the Nafion 212 membrane due to its higher water electro-osmotic drag coefficient than that of the PEMFC with other membranes. Water crossover behavior has been characterized [18,19]. Because the proton conductor in the electrode was Nafion and NF-SPI-NF membranes, the NF-SPI-NF fabricated in this work can avoid direct contact between the SPI membrane and catalyst electrode, and can help decrease interfacial resistance.

3.6. Durability

Fig. 4 shows the diagram of time course versus cell voltage during operation at a constant current density of 0.2 A cm^{-2}. Both the NF-SPI-NF and the Nafion 212 membranes had good durability and operated successfully for 120 h. However, the PEMFC with SPI membrane had the largest decline in cell voltage during operation, leading to the performance stopping of the fuel cell. Performance of the PEMFC with NF-SPI-NF membrane was comparable to that of the EMFC with Nafion 212 membrane, indicating that decreased ohmic loss of the PEMFC with NF-SPI-NF membrane was due to enhance adhesion between the SPI-NF membrane and catalyst electrode. The proton conduction pathway between the SPI-NF membrane and the Nafion binder in the catalyst layer formed properly and was similar to that between the Nafion 212 membrane and Nafion binder. The Nafion layers adhered to both sides of the

Table 2
PEMFC performance of SPI, SPI-NF, and Nafion 212 membranes.

Temperature (°C)	Code	OCV (V)	$V_{1.0}$ (V)[a]	$R_{1.0}$ (mΩ cm^{-2})[a]	$\sigma_{\perp,FC}$ (mS cm^{-1})[b]	W_{max} (mW cm^{-2})
30	SPI	0.94	0.54	0.225	53.3	592
	SPI-NF	0.95	0.55	0.217	55.2	626
	Nafion 212	0.95	0.54	0.219	54.8	620
70	SPI	0.95	0.60	0.0179	67.0	740
	SPI-NF	0.94	0.61	0.0175	68.6	763
	Nafion 212	0.97	0.62	0.0180	66.7	768

[a] At 1 A cm^{-2}.
[b] Assuming that the membrane resistance is approximately equal to the cell resistance at 1 A cm^{-2}.

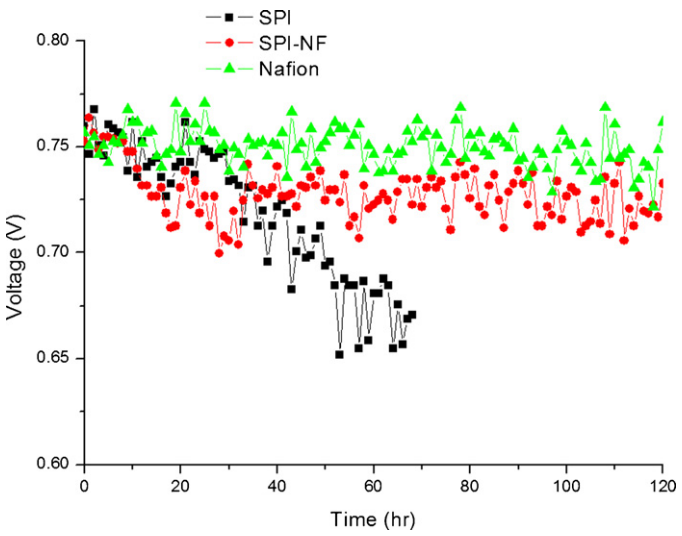

Fig. 4. Fuel cell durability test of a single cell with SPI and SPI-NF membranes with humidified H_2/O_2 at 30 °C.

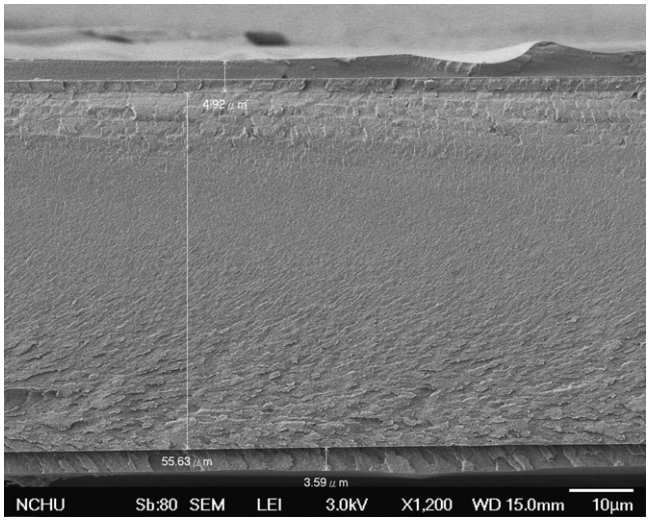

Fig. 5. SEM image of cross-section of the SPI-NF multilayer membrane.

SPI membrane, protecting it from free radical attacks, which may occur during redox reactions. We argue that the proposed method for preparing the SPI membrane coated on either side with a Nafion layer during MEA fabrication is a very effective for achieving long-term stable cell performance.

3.7. Morphology

Fig. 5 shows SEM micrographs of the NF-SPI-NF membrane cross section. The cross-sectional morphology, indicates that the multilayer membrane had three layers. The Nafion layers on each side of the SPI membrane adhered well to the SPI membrane. The thickness of the Nafion layers was uniform.

After the durability test, cells were opened and the partial cross-section of the MEA was examined by SEM. Fig. 6(a) shows the MEA partial cross section of the SPI membrane. There are an interface between the catalyst electrode and the SPI layer due to incompatibility and poor bonding between the Nafion binder and SPI membrane. Fig. 6(b) shows an SEM micrograph of an MEA with NF-SPI-NF membrane. The image shows good adhesion between the catalyst electrode and NF-SPI-NF membrane.

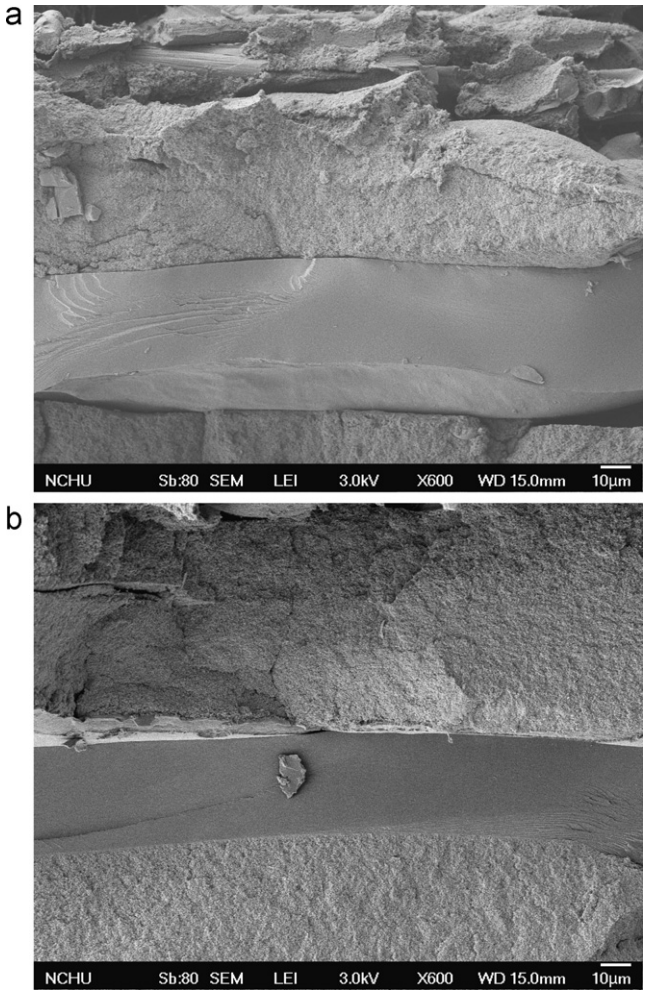

Fig. 6. SEM image of MEA partial cross-section for membranes after durability test: (a) SPI and (b) SPI-NF.

4. Conclusions

In this work, NF-SPI-NF multilayer membranes were successfully prepared by immersing SPAA into the Nafion-coating solution. The NF-SPAA-NF membrane was then thermally imidized via solvent evaporation and an NF-SPI-NF membrane formed. The Nafion layer was securely adhered to the SPI membrane via thermal imidization. The NF-SPI-NF membrane had better proton conductivity than the SPI membrane with the same thickness under the same conditions. The Nafion layer on either side of the SPI membrane effectively enhanced the stability of native SPI. Performance of the PEMFC with NF-SPI-NF membrane was better than that of the PEMFC with SPI membrane, due to better adhesion between the catalyst electrode and membrane.

References

[1] L. Carrette, K.A. Friedrich, U. Stimming, Fuel Cells 1 (2001) 5–39.
[2] B.C.H. Steele, A. Heinzel, Nature 414 (2001) 345–352.
[3] A. Heinzel, V.M. Barragán, J. Power Sources 84 (1999) 70–74.
[4] M.A. Hickner, H. Ghassemi, Y.S. Kim, B.R. Einsla, J.E. McGrath, Chem. Rev. 104 (2004) 4587–4612.
[5] E. Vallejo, G. Pourcelly, C. Gavach, R. Mercier, M. Pineri, J. Membr. Sci. 160 (1999) 127–137.
[6] C. Genies, R. Mercier, B. Sillion, N. Cornet, G. Gebel, M. Pineri, Polymer 42 (2001) 359–373.
[7] S. Besse, P. Capron, O. Diat, G. Gebel, F. Jousse, D. Marsacq, M. Pineri, C. Marestin, R. Mercier, J. New Mater. Electrochem. Syst. 5 (2002) 109–112.
[8] C.H. Lee, S.Y. Lee, Y.M. Lee, J.E. McGrath, Langmuir 25 (2009) 8217–8225.
[9] R. Jiang, H.R. Kunz, J.M. Fenton, J. Electrochem. Soc. 153 (2006) A1554.

[10] L. Wang, B. Yi, H. Zhang, Y. Liu, D. Xing, Z. Shao, Y. Cai, J. Power Sources 164 (2007) 80–85.
[11] K.A. Sung, K.-Y. Cho, W.-K. Kim, J.-K. Park, Electrochim. Acta 55 (2010) 995–1000.
[12] X. Guo, J. Fang, T. Watari, K. Tanaka, H. Kita, K.-i. Okamoto, Macromolecules 35 (2002) 6707–6713.
[13] Z. Hu, Y. Yin, K. Yaguchi, N. Endo, M. Higa, K.-i. Okamoto, Polymer 50 (2009) 2933–2943.
[14] Z. Liang, W. Chen, J. Liu, S. Wang, Z. Zhou, W. Li, G. Sun, Q. Xin, J. Membr. Sci. 233 (2004) 39–44.
[15] X. Ye, H. Bai, W.S.W. Ho, J. Membr. Sci. 279 (2006) 570–577.
[16] R.J. Stanis, M.A. Yaklin, C.J. Cornelius, T. Takatera, A. Umemoto, A. Ambrosini, C.H. Fujimoto, J. Power Sources 195 (2010) 104–110.
[17] Y. Sutou, Y. Yin, Z. Hu, S. Chen, H. Kita, K.-I. Okamoto, H. Wang, H. Kawasato, J. Polym. Sci., Part A: Polym. Chem. 47 (2009) 1463–1477.
[18] K. Yaguchi, K. Chen, N. Endo, M. Higa, K.-i. Okamoto, J. Power Sources 195 (2010) 4676–4684.
[19] K.-i. Okamoto, K. Yaguchi, H. Yamamoto, K. Chen, N. Endo, M. Higa, H. Kita, J. Power Sources 195 (2010) 5856–5861.